Geophys. J. Int. (2008) **173,** 465–472 doi: 10.1111/j.1365-246X.2008.03704.x

A new absolute arrival time data set for Europe

M. L. Amaru,[1]* W. Spakman,[1] A. Villaseñor,[1,2] S. Sandoval[1,3] and E. Kissling[4]

[1]*Department of Earth Sciences, Utrecht University, Budapestlaan* 4, 3584CD *Utrecht, The Netherlands. E-mail: amaru@geo.uu.nl*
[2]*Institute of Earth Sciences "Jaume Almera", CSIC, Barcelona, Spain*
[3]*Geofisica Aplicada Consultores, Madrid, Spain*
[4]*Institute of Geophysics, ETH Hönggerberg, Zürich, Switzerland*

Accepted 2007 December 3. Received 2007 December 3; in original form 2007 March 14

SUMMARY

The main aim of this study is to create a data set of accurate absolute arrival times for stations in Europe which do not report to the International Seismological Centre (ISC). Waveforms were obtained from data centres and temporary experiments and a semi-automatic picking method was applied to determine absolute arrival times for *P* and *S* phases. 85 000 arrival times were picked whose distribution of residuals shows generally low standard deviations on the order of 0.5–0.7 s. Furthermore, mean teleseismic station residuals reflect the properties of the underlying crust and uppermost mantle. Comparison to ISC data for matching event-station-phase combinations also confirms the good quality of the new absolute arrival time picks. Most importantly, this data set complements the ISC data as it fills regional data coverage gaps in Europe.

Key words: Body waves; Europe.

1 INTRODUCTION

Arrival times are routinely reported by many seismological networks to the International Seismological Centre (ISC), resulting in bulletins of millions of arrival times since 1964. Clearly, a wealth of information can be gained from these data regarding the Earth's interior for example by application of traveltime tomography. However, the reporting stations are not distributed equally over the globe therefore leaving gaps, in particular, in the oceans and stable cratonic regions. Furthermore, the quality of these data, which are mostly handpicked, varies greatly (Röhm *et al.* 1999).

Besides stations included in arrival time bulletins, a large number of seismic stations exist whose waveforms are not used routinely but are sent to data centres for digital storage. For many events included in these waveforms, arrival times were either not picked at all or only with limitations (e.g. a restricted period in time or limited epicentral distance range).

Another valuable source of data is provided by temporary experiments. To fill the geographical gaps, many regional experiments were carried out during the last 15–20 yr where spatially dense temporary networks were placed in the field for several months. Often, arrival times for events registered at those arrays were only picked relatively. That means, not the arrival time of a phase onset was determined but the arrival time of the first maximum or minimum after the onset. This procedure has the advantage that observational errors due to high noise levels can be reduced but as a major disadvantage, arrival times are only obtained with respect to the unknown mean network arrival time for a specific event. Therefore, they cannot be used for event relocation or to obtain absolute velocity information on the crust and mantle below the array. Consequently, obtaining absolute arrival times for events recorded at such stations which do not report arrival times to the ISC can provide new detailed information for high-resolution traveltime tomography.

Besides using additional stations, the picks should also be of a consistent good quality as erroneous picks will affect or overprint velocity structures which would otherwise be imaged in traveltime tomography. Generally, hand picks are considered to give the best quality but for large data sets this approach is not feasible. However, advanced automatic picking techniques can be applied when many waveforms are recorded for a single event which provide very accurate picks.

The aim of this study is to present such a data set of absolute arrival times for Europe. This data set provides high quality picks of previously unused waveforms and can, for instance, be combined with the ISC arrival times for traveltime tomography. To ensure a good picking quality for a large number of waveforms we apply a recently developed two-step semi-automatic phase picker. With our approach, we focus on Europe where many temporary experiments have taken place and where data centres provide a large source of additional waveforms from various digital networks in Europe.

2 DATA

During the past 15 yr large teleseismic experiments were conducted in Europe where spatially dense seismograph arrays were placed in the field for several months. Data from such experiments

*Now at: Chevron Energy Technology Company, Houston, TX, USA.

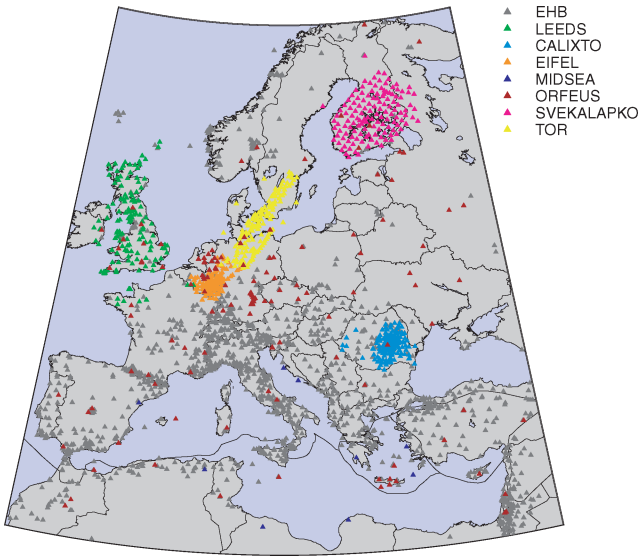

Figure 1. Station locations. The different colours denote to which network/data source the stations belong.

were obtained as waveforms from the CALIXTO, EIFEL, MIDSEA, SVEKALAPKO and TOR experiment. Another data collection (named 'Leeds' data set hereafter) was provided by the University of Leeds, UK (Arrowsmith 2003) and the Observatories and Research Facilities for EUropean Seismology (ORFEUS) data centre forms a further important source of waveforms. A map of all station locations is displayed in Fig. 1.

2.1 Leeds data set

This waveform collection comprises 150 stations from the British Geological Survey (BGS), Dublin Institute for Advanced Studies (DIAS) and Laboratoire de Détection et de Géophysiqe, France (LDG) seismic networks. Many of these stations did not report arrival times to the ISC on a regular basis. The data set contains recordings from the period 1993–2001. It was used so far only for classic teleseismic traveltime tomography with relative arrival time picks (Arrowsmith 2003; Arrowsmith *et al.* 2005) to investigate the relation between asthenosphere, lithosphere and crust beneath the British Isles. We used the waveforms as provided to us by S. Arrowsmith (personal communication, 2004).

2.2 CALIXTO

The Carpathian Arc LIthosphere X-TOmography (CALIXTO) experiment was carried out to investigate the lithosphere/ asthenosphere structure of the Vrancea zone (southeast Carpathians) known for its strong and localized seismicity. From 1999 May to November, 110 mobile stations were placed in the field in Romania. The data set was supplemented by recordings from 18 permanent stations in Romania (see Wenzel *et al.* 1998, for details). Among the published tomography studies about the CALIXTO experiment are teleseismic *P* tomography studies using relative traveltime residuals (Martin & Ritter 2005; Martin *et al.* 2006), an upper crustal absolute *P* tomography (Landes *et al.* 2004) and a study using handpicked absolute *P* arrival times by Weidle *et al.* (2005). However, absolute arrival times were neither picked for *S* waves nor for the entire set of local and regional events.

2.3 EIFEL

The EIFEL project was conducted to investigate the Quarternary volcanism in the Eifel and a possible mantle plume as its origin. Between 1997 November and 1998 June, 158 stations were operated in the Eifel and surrounding regions. Ritter *et al.* (2000) give an overview of the experiment. Among studies about this experiment are a receiver function study (Grunewald *et al.* 2001), a teleseismic *P* tomography (Ritter *et al.* 2001) and a teleseismic *S* tomography study (Keyser *et al.* 2002) both using relative traveltime residuals.

2.4 MIDSEA

The Mantle Investigation of the Deep Suture between Eurasia and Africa (MIDSEA) project was performed to fill gaps in the Mediterranean area where no broad-band recordings existed before and should therefore improve images of the lithosphere and mantle beneath the Mediterranean region (Van der Lee *et al.* 2001). Registrations from 10 stations were available via ORFEUS. These stations had been placed in the field for 1–2 yr during the period 1999 June–2002 April. Among studies about this project are a receiver function study (Van der Meijde *et al.* 2003), a surface wave tomography study (Marone *et al.* 2003) and a shear wave splitting analysis (Schmid *et al.* 2004). For this data set, absolute arrival times were not picked.

2.5 SVEKALAPKO

The SVEcofennian-KArelian-LAPland-KOla (SVEKALAPKO) project was carried out in Finland with the aim to get a better understanding of the formation of the oldest continents, namely the core of the Karelian province of Archean age (2.6 Ga). 128 mobile stations were placed in the field from 1998 August to 1999 May. The data set was completed by recordings from 15 permanent stations (see Bock & the SVEKALAPKO Seismic Tomography Working Group 2001, for experiment details). Among studies about this experiment are a receiver function study (Alinaghi *et al.* 2003), a teleseismic *P* tomography study (Sandoval *et al.* 2003, 2004a), a surface wave tomography study (Bruneton *et al.* 2004) and a local tomography study (Yliniemi *et al.* 2004). Only for the local study, absolute arrival times were used.

2.6 TOR

For the Teleseismic Tomography across the Tornquist Zone in Germany–Denmark–Sweden (TOR) experiment, 120 stations were placed in South Sweden, Denmark and North Germany from 1996 July to 1997 August to image the Tornquist zone, that separates the Baltic shield from the younger (Phanerozoic) parts of Central Europe, in greater detail than before. Many studies already exist for this experiment using a range of seismological methods. Besides an overview of the experiment given by Gregersen *et al.* (2002), among the studies are a teleseismic *P* tomography (Arlitt *et al.* 1999), non-linear *P* and *S* tomography studies (Shomali *et al.* 2006; Voss *et al.* 2006), receiver function studies (Gossler *et al.* 1999; Wilde-Piórko *et al.* 2002; Alinaghi *et al.* 2003) and anisotropy analyses (Wylegalla & TOR Working Group 1999; Plomerova & TOR Working Group 2002). However, none of the named studies used absolute traveltimes.

2.7 ORFEUS

The ORFEUS Data Center provides the biggest data set particularly picked for our study. Their archive contains seismograms from the years 1988 to 2000 for stations of the European digital seismometer network. Out of 160 stations available in these archives, 53 stations had not been used previously and for 40 stations we were able to fill gaps where traveltimes had only been reported for limited epicentral distance ranges or for a limited period in time. In total, for the earthquakes for which we picked arrival times, 109 500 records went into the phase picking process. However, a significant number of records were discarded, in particular, for earthquakes with a low signal-to-noise ratio at larger epicentral distances.

3 METHOD

The data described above were obtained from the individual sources as waveform recordings. Since the main interest of this study are the arrival times, those waveforms were processed further. They were either obtained already sorted by events or, if necessary, the events were selected from the EHB catalogue (Engdahl *et al.* 1998), a reprocessed version of the ISC bulletins, using within Europe earthquakes with $m_b > 4.5$ and for teleseismic events earthquakes with $m_b > 5.5$. As the seismograms were provided in various data formats, they were converted by us to the common format SAC (Goldstein *et al.* 2003). Since the stations were equipped with different types of sensors which are sensitive in different frequency ranges, the recordings were restituted to simulate the short period World Wide Standardized Seismographic Network (WWSSN) sensor with a dominant frequency around 1 Hz. Besides *P*-wave arrivals for events in all distance ranges, also *S*-wave arrivals were picked for the CALIXTO data set. In those cases, the recordings were restituted with a Wiechert sensor with a dominant frequency of 0.1 Hz and continuing high amplification towards higher frequencies to account for the lower frequencies of *S*-waves. As a next step, the waveforms were bandpass filtered according to the epicentral distance of the registered phase and the phase type (see Table 1). Theoretical traveltimes were computed for all recordings in the Earth reference model ak135 (Kennett *et al.* 1995) to choose appropriate time windows for the traveltime picking. The horizontal N–S and E–W oriented components of the CALIXTO recordings were rotated to the radial and transverse components according to the theoretical backazimuth of the events to allow picking of the SV and SH arrivals, respectively.

Because of the large number of waveforms (184 000 waveforms), hand-picking was not feasible anymore. Therefore, the picking of the arrival times was carried out with a semi-automated picking software developed by Sandoval *et al.* (2004b). The picking was performed per event with a two-step algorithm consisting of an STA/LTA picking method and a cross-correlation to ensure a good picking quality. First, the STA/LTA algorithm of Earle & Shearer (1994) was applied. This algorithm is based on a short-term-average to long-term-average ratio taken along an envelope function of the seismogram and returns the absolute arrival time as a result. Subsequently, the picks were grouped regionally dividing the area covered by stations into equally sized subregions and a reference station with a high signal-to-noise ratio was selected manually for each region. As a second step, the reference waveforms were cross-correlated with each other for consistency between the regions. Afterwards, the waveforms within each region were cross-correlated with the reference station to improve the STA/LTA pick. This method was applied for picking of the CALIXTO, EIFEL and SVEKALAPKO experiments.

Later on, the picking procedure was modified to represent in its final version an implementation of the adaptive stacking algorithm of Rawlinson & Kennett (2004). It was applied to the Leeds, MIDSEA, ORFEUS and TOR data sets. Instead of cross-correlation, an adaptive stacking was applied to clusters of stations as this method is more robust concerning waveform variability than cross-correlation techniques. Furthermore, unlike before it does not require input from the user to choose reference waveforms which would have been too time-consuming for larger data sets. With this method, all waveforms were initially aligned with respect to their theoretical traveltime and stacked. They were shifted with respect to the stack to iteratively maximize the stack. As a result, the traveltime residual of each phase relative to its theoretical traveltime was obtained and an error estimate was computed via the misfit between the individual waveforms and the stacked signal.

Additionally, as grouping by equally sized subregions is not the optimum approach for wide-spread station locations as the ORFEUS stations, a cluster analysis was performed to group stations with similar waveforms for the adaptive stacking according to their epicentral distance and azimuth. An initial number of clusters was defined depending on the minimum and maximum lateral extent of the station distribution. As further input, the method required the minimum and maximum number of stations per cluster. The minimum number of stations should be large enough to ensure a high signal-to-noise ratio of the stacked waveform yet the maximum number of stations should be low enough to avoid distortion of the stacked waveforms due to varying waveforms at widely spread stations. For clusters with less than the minimum number of required stations, the stations were reassigned to the neighbouring clusters. Clusters with more than the maximum number of stations were split into two clusters.

Subsequent to the adaptive stacking performed on each cluster of stations, the STA/LTA picker (Earle & Shearer 1994) was applied to the stacked waveform assuming that the frequency content within each cluster is similar to allow for accurate picking of the phase onset on the stack. Finally, absolute arrival times were computed for each station from the combination of STA/LTA pick and relative station residuals.

As this picking process is applied to each cluster independently, it may result in offsets between the absolute picks of the stacked waveforms, in particular between distant clusters. Both, to avoid those offsets and to get an impression of the variability of the stacks within the different clusters, they were aligned visually according to their STA/LTA pick and the graphical user interface enables the user to change or remove picks which display an offset compared to the other picks.

As a final quality check, all traveltime residuals were displayed geographically similar to Fig. 4 (right-hand panel) to identify and remove remaining potential outliers.

Such methods as described above work well if the waveforms within a group/cluster are similar to each other but work less well if waveforms change rapidly with distance as can be the case for example for local events. Then, the graphical interface of the traveltime picker allows for user input to pick the arrival times by hand.

Table 1. Bandwidth of the applied bandpass filter with regard to phase type and epicentral distance.

Δ	<10°	10°–30°	>30°
P	0.5–6.0 Hz	0.3–4.0 Hz	0.2–2.0 Hz
S	0.1–5.0 Hz	0.01–2.0 Hz	0.01–2.0 Hz

Table 2. Summary of the obtained arrival time picks.

Data set	Picks	Events	Distance range
Leeds	5228 (P)	64	32°–157°
CALIXTO	4361 (P)	208	0°–156°
	1830 (SV)	103	0°–86°
	1909 (SH)	103	0°–86°
EIFEL	6124 (P)	87	7°–161°
MIDSEA	733 (P)	256	0°–160°
ORFEUS	54646 (P)	2054	0°–170°
SVEKALAPKO	5128 (P)	101	21°–145°
TOR	5113 (P)	148	1°–161°

4 RESULTS

In total, 85 000 absolute arrival time picks were obtained with an estimated picking error of 0.20–0.30 s. Table 2 gives a more detailed overview of the number of picks. All residuals used and displayed in this study are computed with respect to ak135. As is shown in Fig. 2, the residuals (observed—theoretical traveltime) are centred around −0.11 s with a standard deviation of 0.86 s appropriate for a data set that contains information about many different geological settings. The solid black line in Fig. 2 represents the best-fitting Gaussian curve with a standard deviation of 0.69 s. Towards bigger residuals, the observed data do not follow a normal distribution but show a broader tail. This effect is mainly attributed to errors in the data set (for example, event mislocation or picking errors) but also to 3-D velocity structures along the ray path (e.g. Pulliam *et al.* 1993; Röhm 1999).

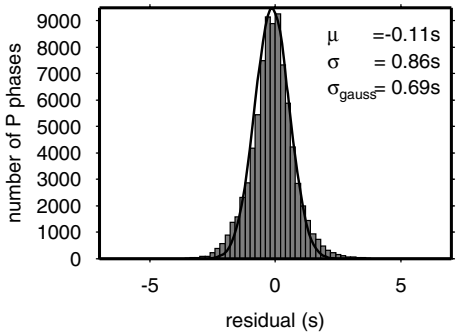

Figure 2. Histogram of the *P* residuals (with respect to ak135) for the newly picked data. The solid line indicates the best-fitting Gaussian function.

Generally, rays from teleseismic events recorded at a dense station array take approximately the same path through the Earth except for the part directly beneath the array. Therefore, their traveltime differences for each event reflect the velocity differences of the crust and lithosphere beneath the array. Two examples which indicate the high quality of the obtained picks are illustrated in Figs 3 and 4. In Fig. 3, an event beneath Sumatra registered at the EIFEL array is displayed. It shows highest residuals in the centre of the array and west of it indicating the lower velocities directly beneath the Eifel. In Fig. 4, the registered waveforms and obtained traveltime residuals for an event in the eastern Sea of Japan registered at the TOR array are shown. A transition can be observed from negative residuals in the north due to the high velocities of the Baltic shield across the Tornquist zone to higher residuals related to the lower velocities of the younger parts of central Europe.

The semi-automatic picker works best for teleseismic *P* phases since waveforms from teleseismic events recorded at a regional/local station network vary only gradually while rapid waveform changes can be expected for local recordings due to crustal heterogeneities and greatly varying incidence angles. Therefore, even though data for all distance ranges were picked, for the remainder of this paper, focus will be on *P* arrival times obtained for teleseismic events ($\Delta > 28°$). Computing the mean of all teleseismic residuals obtained at a single station will mainly reflect the regional velocity variations underneath the stations as for a wide azimuthal coverage of epicentral regions source effects and contributions of the paths further away from the station will diminish. In Fig. 5, the mean teleseismic station residuals of the new data and their standard deviations are presented (upper and lower right-hand side, respectively). For comparison, the mean teleseismic residuals and standard deviations of the ISC bulletins are displayed on the upper and lower left-hand side.

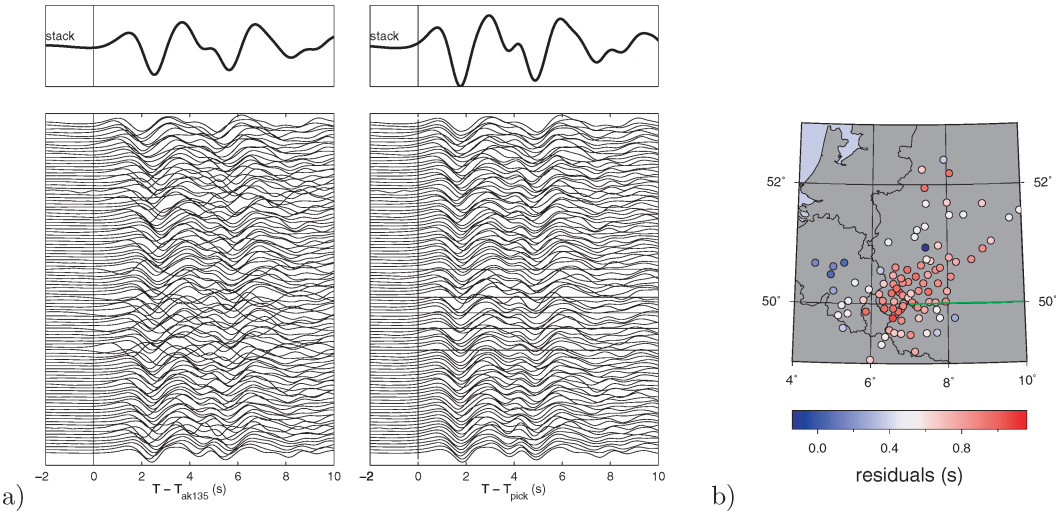

Figure 3. (a) Example of processed waveforms aligned with respect to the theoretical (left-hand side) and picked arrival time (right-hand side) for an event beneath Sumatra (1998 April 1 17:56:21.89, 0.564°S, 99.195°E, $z = 32.0$ km, $m_b = 6.0$) recorded at the EIFEL array. Traces without a picked arrival time are indicated by flat lines in the right-hand panel. The stacks plotted above the waveforms are the sum of all waveforms aligned with regard to the theoretical and picked arrival time, respectively. (b) Displayed are the corresponding residuals with respect to ak135 ($T_{\mathrm{pick}} - T_{\mathrm{ak135}}$). The green line indicates the direction of incidence of the wave front.

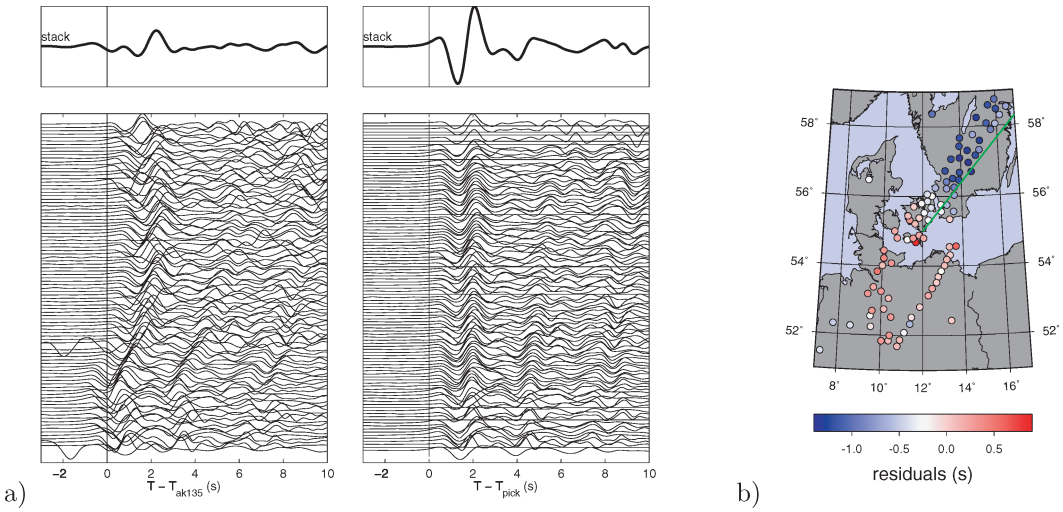

Figure 4. (a) Example of processed waveforms aligned with respect to the theoretical (left-hand side) and picked arrival time (right-hand side) for an event in the eastern Sea of Japan (1996 December 22 14:53:29.07, 43.240°N, 138.886°E, $z = 227.0$ km, $m_b = 5.9$) recorded at the TOR array. Traces without a picked arrival time are indicated by flat lines in the right-hand panel. The stacks plotted above the waveforms are the sum of all waveforms aligned with regard to the theoretical and picked arrival time, respectively. (b) Displayed are the corresponding residuals with respect to ak135 ($T_{\rm pick} - T_{\rm ak135}$). The green line indicates the direction of incidence of the wave front.

Negative residuals are found beneath the SVEKALAPKO array and the northern part of the TOR array reflecting the high velocities of the Baltic shield. The residuals become positive at the southern part of the TOR array due to the lower velocities of the underlying lithosphere. The Eifel region shows in the central part slightly positive residuals related with the lower velocities underneath it while they are lower in the surrounding regions. For the Leeds data set, generally small residuals are found with the most negative residuals in the Central Highlands region possibly caused by high velocities of remnants of a subducted oceanic plate (Arrowsmith 2003, and reference therein). The CALIXTO array shows positive residuals in the bend zone of the southeast Carpathians and in the Transylvanian and Focsani basins. Negative residuals are found towards the northeast on the East European Platform and in the southwestern part of the seismic array. Overall, 53 of the 160 stations in the ORFEUS archive did not report arrival times to the ISC, in particular Network of Autonomously Recording Seismographs stations (NARS, see e.g. Paulssen *et al.* (1990, 2000)) and about 40 more stations either reported only local and regional arrival times to the ISC or not for the entire period of operation. Picking of arrival times from the rest of the stations did not consume much extra time due to the applied picking method. The ORFEUS stations on the East European Platform display negative residuals due to the fast velocities of the old cratonic material beneath it while for example the stations in the Netherlands show positive residuals.

A comparison of the new data with the mean teleseismic residuals of the EHB catalogue (originating from the ISC bulletins) shows similarities but due to the locally denser station distribution regional variations can be seen in more detail as, for example, across the Tornquist zone.

The standard deviation of the new teleseismic residuals are generally low around 0.5–0.7 s except for regions where the residuals show a strong azimuthal dependence (e.g. TOR—many events either from north–northeast along array direction or perpendicular to the array from east–southeast, CALIXTO—complex tectonic structure due to collisional setting, deep sediment basins) or concerning the highest standard deviations where only few teleseismic arrival time picks with greater variation exist. Nevertheless, the scatter of residuals is much lower than for most of the ISC data indicating the high quality of the data set.

As a final inspection of the new picks, identical teleseismic event-station-phase pairs were retrieved from the EHB catalogue and compared to the new picks. Approximately 13 500 such pairs could be found mainly from the ORFEUS catalogue but also for stations of the other data sets. As displayed in Fig. 6, the new residuals are on average 0.08 s faster with a standard deviation of 0.74 s for the difference between the residuals. The mean baseline shift of 0.08 s between ISC and newly picked data may be caused by using different frequency ranges for filtering or by simulating different instrument responses. We used standard techniques to simulate a short-period sensor and common values for the filtering process (*cf.* Section 3). However, we cannot estimate the impact of these effects as the ISC data set is very heterogeneous concerning processing at the stations and networks and often information about the processing parameters does not exist. The standard deviation represents the difference in error between the individual ISC and newly picked delay times ($d_{\rm ISC}$ and $d_{\rm NEW}$, respectively), as the difference in residuals corresponds to the difference in picking errors if identical phases are picked:

$$d_{\rm ISC} = d + \epsilon_{\rm ISC} \tag{1}$$

$$d_{\rm NEW} = d + \epsilon_{\rm NEW} \tag{2}$$

$$\Rightarrow d_{\rm ISC} - d_{\rm NEW} = \epsilon_{\rm ISC} - \epsilon_{\rm NEW}, \tag{3}$$

where d is the residual without picking errors, $\epsilon_{\rm ISC}$ and $\epsilon_{\rm NEW}$ are the picking errors.

However, part of the standard deviation obtained for the distribution of $(d_{\rm ISC} - d_{\rm NEW})$ may be attributed to different phase associations. That means phases identified in our picking process as *P*, for example, might be identified as PcP in the EHB catalogue when the theoretical arrival times are similar, resulting in the comparison of essentially different arrivals. Though this effect should be small as we used only first arrivals for the comparison and the picks were associated accordingly, it will still add to the overall standard deviation. Therefore, we can only estimate that a standard deviation of 0.74 s for the distribution of $(d_{\rm ISC} - d_{\rm NEW})$ measurements is in

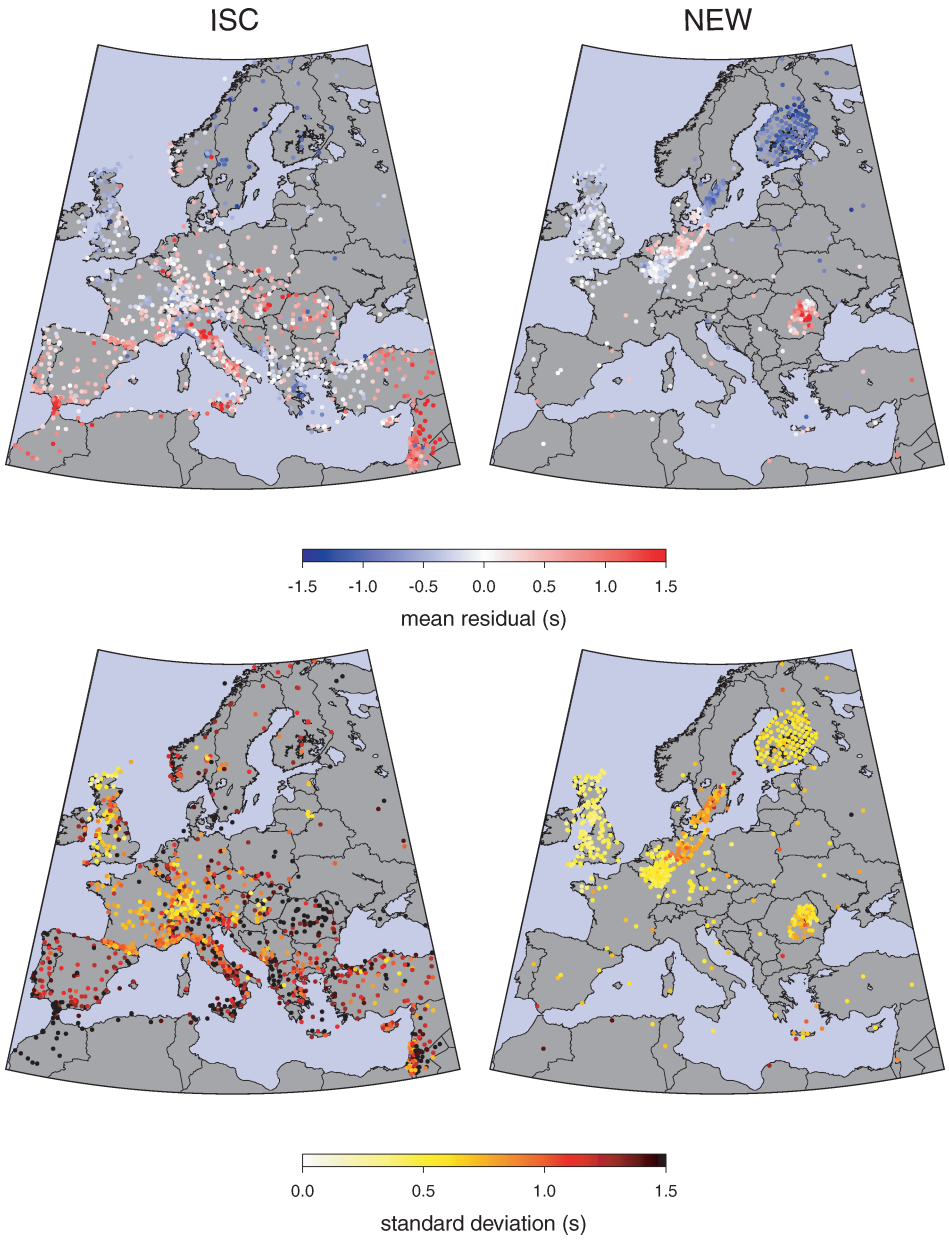

Figure 5. Mean teleseismic *P* traveltime residuals per station for the EHB data set (upper left-hand side) and the new data (upper right-hand side) and standard deviation per station for the EHB data set (lower left-hand side) and the new data (lower right-hand side). All residuals are computed with respect to the reference model ak135. Only stations with more than 15 recordings are displayed.

agreement with a picking error on the order of 0.3 s for the newly picked data and using the estimate of Gudmundsson *et al.* (1990) of $\sigma \approx 0.5$ s for random errors in teleseismic ISC residuals.

Picking of SV and SH arrival times from the CALIXTO experiment showed that *S* phases required significantly more tuning of the picker parameters and user input using the method described in Section 3. In addition, horizontal component recordings were not available for all data sets and stations. Therefore, we refrained from picking *S* phases for other data sets.

5 CONCLUSIONS

The main objective of this study was to obtain accurate arrival time picks for stations within Europe which did not report to the ISC and to fill data gaps in regions with few stations. Waveforms were provided by spatially dense temporary arrays and data centres in Europe. These waveforms were then pre-processed and absolute arrival times picked with the semi-automatic phase picker of Sandoval *et al.* (2004b). Analyses of the picks show their high quality and that they contain significant information on the geologic properties of crust and uppermost mantle directly beneath the stations. Therefore, the new data set can be combined with the ISC data for global traveltime tomography to obtain a high-resolution velocity model of crust and mantle beneath Europe in particular beneath the dense station arrays. Furthermore, this study shows where lack of data/stations is still greatest (e.g. parts of East Europe or Scandinavia). For future research, valuable information could also be gained from near real time picking of the Virtual European Broadband Seismograph Network (VEBSN) as gradually more waveforms become available in

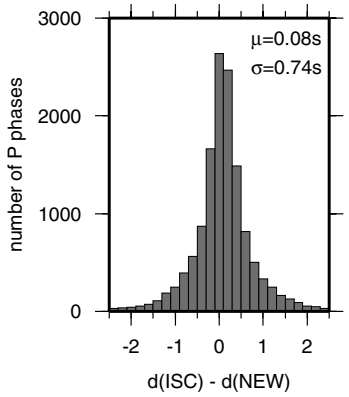

Figure 6. Histogram of the differences between residuals of the EHB data set and the newly picked arrival time data set for matching station-event-phase combinations.

near real time for stations which do not report to the ISC so far. The new arrival time picks are made available on the ORFEUS website (http://orfeus-eu.org).

ACKNOWLEDGMENTS

We thank ORFEUS, GEOFON, Stephen Arrowsmith, the CALIXTO, EIFEL, MIDSEA, SVEKALAPKO and TOR working groups for providing the data used in this study and ORFEUS for storage and access to the new traveltime data set through their websites. We are grateful to T. Becker, S. Godey and an anonymous reviewer for helpful comments and suggestions. This project was funded by ISES (Netherlands Research Centre for Integrated Solid Earth Science).

REFERENCES

Alinaghi, A., Bock, G., Kind, R., Hanka, W., Wylegalla, K. & TOR and SVEKALAPKO Working Group, 2003. Receiver function analysis of the crust and upper mantle from the North German Basin to the Archaean Baltic Shield, *Geophys. J. Int.,* **155,** 641–652.

Arlitt, R., Kissling, E., Ansorge, J. & TOR, Working Group, 1999. Three-dimensional crustal structure beneath the TOR array and effects on teleseismic wavefronts, *Tectonophysics,* **314,** 309–319.

Arrowsmith, S.J., 2003. A tomographic investigation of upper mantle processes beneath the British Isles, *PhD thesis*, University of Leeds, UK.

Arrowsmith, S.J., Kendall, M., White, N., VanDecar, J.C. & Booth, D.C., 2005. Seismic imaging of a hot upwelling beneath the British Isles, *Geology,* **33,** 345–348.

Bock, G. & the, SVEKALAPKO Seismic Tomography Working Group, 2001. Seismic probing of Archaean and Proterozoic Lithosphere in Fennoscandia, *EOS, Trans. Am. Geophys. Un.,* **82,** 50, 621, 628–629.

Bruneton, M. *et al.*, 2004. Complex lithospheric structure under the central Baltic Shield from surface wave tomography, *J. geophys. Res.,* **109,** B10303.

Earle, P.S. & Shearer, P.M., 1994. Characterization of Global Seismograms Using an Automatic-Picking Algorithm, *Bull. seism. Soc. Am.,* **84**(2), 366–376.

Engdahl, E.R., van der Hilst, R.D. & Buland, R.P., 1998. Global teleseismic earthquake relocation with improved travel times and procedures for depth determination, *Bull. seism. Soc. Am.,* **88**(3), 722–743.

Goldstein, P., Dodge, D., Firpo, M. & Minner, L., 2003. SAC2000: Signal processing and analysis tools for seismologists and engineers, in *The IASPEI International Handbook of Earthquake and Engineering,* eds W.H.K. Lee, H., Kanamori, P.C. Jennings & C. Kisslinger, Academic Press, London.

Gossler, J., Kind, R., Sobolev, S., Kämpf, H., Wylegalla, K., Stiller, M. & TOR, Working Group, 1999. Major crustal features between the Harz Mountains and the Baltic Shield derived from receiver functions, *Tectonophysics,* **314,** 321–333.

Gregersen, S., Voss, P. & TOR, Working Group, 2002. Summary of project TOR: delineation of a stepwise, sharp, deep lithosphere transition across Germany–Denmark–Sweden, *Tectonophysics,* **360**(1–4), 61–73.

Grunewald, S., Weber, M. & Kind, R., 2001. The upper mantle under Central Europe: indications for the Eifel plume, *Geophys. J. Int.,* **147,** 1–17.

Gudmundsson, O., Davies, J.H. & Clayton, R.W., 1990. Stochastic analysis of global traveltime data: mantle heterogeneity and random errors in the ISC data, *Geophys. J. Int.,* **102,** 25–43.

Kennett, B.L.N., Engdahl, E.R. & Buland, R., 1995. Constraints on seismic velocities in the Earth from traveltimes, *Geophys. J. Int.,* **122,** 108–124.

Keyser, M., Ritter, J. & Jordan, M., 2002. 3D shear-wave velocity structure of the Eifel plume, Germany, *Earth Planet. Sci. Lett.,* **203,** 59–82.

Landes, M., Fielitz, W., Hauser, F., Popa, M. & CALIXTO group, 2004. 3-D upper-crustal tomographic structure across the Vrancea seismic zone, Romania, *Tectonophysics,* **382,** 85–102.

Marone, F., van der Meijde, M., van der Lee, S. & Giardini, D., 2003. Joint inversion of local, regional and teleseismic data for crustal thickness in the Eurasia-Africa plate boundary region, *Geophys. J. Int.,* **154,** 499–514.

Martin, M. & Ritter, J.R.R., 2005. High-resolution teleseismic body-wave tomography beneath SE Romania—I. Implications for three-dimensional versus one-dimensional crustal correction strategies with a new crustal velocity model, *Geophys. J. Int.,* **162,** 448–460.

Martin, M., Wenzel, F. & CALIXTO working group, 2006. High-resolution teleseismic body wave tomography beneath SE-Romania—II. Imaging of a slab detachment scenario, *Geophys. J. Int.,* **164,** 579–595.

Paulssen, H., der Lee, S.V. & Nolet, G., 1990. The NARS-Netherlands Project, *IRIS Newsletter,* **9**(4), 1–2.

Paulssen, H., Bukchin, B.G., Emelianov, A.P., Lazarenko, M., Muyzert, E., Snieder, R. & Yanovskaya, T.B., 2000. The NARS-DEEP project, *Tectonophysics,* **313,** 1–8.

Plomerova, J. & TOR, Working Group, 2002. Seismic anisotropy of the lithosphere around the Trans-European Suture Zone (TESZ) based on teleseismic body-wave data of the Tor experiment, *Tectonophysics,* **360,** 89–114.

Pulliam, R.J., Vasco, D.W. & Johnson, L.R., 1993. Tomographic inversions for mantle P-wave velocity structure based on the minimization of l^2 and l^1 norms of international seismological centre travel time residuals, *J. Geophys. Res.,* **98**(B1), 699–734.

Rawlinson, N. & Kennett, B.L.N., 2004. Rapid estimation of relative and absolute delay times across a network by adaptive stacking, *Geophys. J. Int.,* **157**, 332–340.

Ritter, J.R.R., Achauer, U., Christensen, U.R. & the, Eifel Plume Team, 2000. The teleseismic tomography experiment in the Eifel region, Central Europe: DESIGN and first results, *Seism. Res. Lett.,* **71,** 437–443.

Ritter, J., Jordan, M., Christensen, U. & Achauer, U., 2001. A mantle plume below the Eifel volcanic fields, Germany, *Earth planet. Sci. Lett.,* **186,** 7–14.

Röhm, A., 1999. Statistical properties of travel time measurements and the structure of the Earth's mantle, *PhD thesis*, Universiteit Utrecht, The Netherlands.

Röhm, A., Trampert, J., Paulssen, H. & Snieder, R., 1999. Bias in reported seismic arrival times deduced from the ISC Bulletin, *Geophys. J. Int.,* **137,** 163–174.

Sandoval, S., Kissling, E., Ansorge, J. & the, SVEKALAPKO Seismic Tomography Working Group, 2003. High-resolution body wave tomography beneath the SVEKALAPKO array: I. A priori three-dimensional crustal model and associated traveltime effects on teleseismic wave fronts, *Geophys. J. Int.,* **153,** 75–87.

Sandoval, S., Kissling, E., Ansorge, J. & the, SVEKALAPKO STWG, 2004a. High-resolution body wave tomography beneath the SVEKALAPKO array: II. Anomalous upper mantle structure beneath the central Baltic Shield, *Geophys. J. Int.,* **157,** 200–214.

Sandoval, S., Villasenor, A., Spakman, W., Benz, H.M. & Earle, P., 2004b. Automatic analysis of ANSS waveform data in near real time, *Geophys. Res. Abstr.,* **6,** 00322.

Schmid, C., van der Lee, S. & Giardini, D., 2004. Delay times and shear wave splitting in the Mediterranean region, *Geophys. J. Int.,* **159**(1), 275–290.

Shomali, Z.H., Roberts, R.G., Pedersen, L.B. & TOR, Working Group, 2006. Lithospheric structure of the Tornquist Zone resolved by nonlinear P and S teleseismic tomography along the TOR array, *Tectonophysics,* **416,** 133–149.

Van der Lee, S. *et al.*, 2001. Eurasia-Africa plate boundary region yields new seismographic data, *EOS, Trans. Am. Geophys. Un.,* **82**(51), 637, 645–646.

Van der Meijde, M., Marone, F., Giardini, D. & van der Lee, S., 2003. Seismic evidence for water deep in Earth's upper mantle, *Science,* **300,** 1556–1558.

Voss, P., Mosegaard, K., Gregersen, S. & TOR, Working Group, 2006. The Tornquist Zone a north east inclining lithospheric transition at the south western margin of the Baltic Shield: revealed through a nonlinear teleseismic tomographic inversion, *Tectonophysics,* **416,** 151–166.

Weidle, C., Widiyantoro, S. & CALIXTO, Working Group, 2005. Improving depth resolution of teleseismic tomography by simultaneous inversion of teleseismic and global P-wave traveltime data-application to the Vrancea region in Southeastern Europe, *Geophys. J. Int.,* **162,** 811–823.

Wenzel, F., Achauer, U., Enescu, D., Kissling, E., Russo, R., Mocanu, V. & Musacchio, G., 1998. Detailed look at final stage of plate break-off is target of study in Romania, *EOS, Trans. Am. Geophys. Un.,* **79,** 589, 592–594.

Wilde-Piórko, M., Grad, M. & TOR, Working Group, 2002. Crustal structure variation from the Precambrian to Palaeozoic platforms in Europe imaged by the inversion of teleseismic receiver functions—project TOR, *Geophys. J. Int.,* **150,** 261–270.

Wylegalla, K. & TOR, Working Group, 1999. Anisotropy across the Sorgenfrei–Tornquist zone from shear wave splitting, *Tectonophysics,* **314,** 335–350.

Yliniemi, J., Kozlovskaya, E., Hjelt, S.-E., Komminaho, K., Ushakov, A. & SVEKALAPKO, Seismic Tomography Working Group, 2004. Structure of the crust and uppermost mantle beneath southern Finland revealed by analysis of local events registered by the SVEKALAPKO seismic array, *Tectonophysics,* **394**(1–2), 41–67.